



Air-sea CO₂ fluxes and the controls on ocean surface pCO₂ seasonal variability in the coastal and open-ocean southwestern Atlantic Ocean: a modeling study

R. Arruda¹, P. H. R. Calil¹, A. A. Bianchi^{2,3}, S. C. Doney⁴, N. Gruber⁵, I. Lima⁴, and G. Turi^{5,a}

¹Laboratório de Dinâmica e Modelagem Oceânica (DinaMO), Instituto de Oceanografia, Universidade Federal do Rio Grande, Rio Grande, RS, Brazil

²Departamento de Ciencias de la Atmósfera y los Océanos, Universidad de Buenos Aires, Buenos Aires, Argentina

³Departamento Oceanografía, Servicio de Hidrografía Naval, Av. Montes de OCA2124-Buenos Aires, Argentina

⁴Department of Marine Chemistry and Geochemistry, Woods Hole Oceanographic Institution, Woods Hole, MA, USA

⁵Institute of Biogeochemistry and Pollutant Dynamics, ETH Zurich, Zurich, Switzerland

^anow at: CIRES, University of Colorado at Boulder, and NOAA/ESRL, Boulder, CO, USA

Correspondence to: R. Arruda (cadoarruda@gmail.com)

Received: 5 March 2015 – Published in Biogeosciences Discuss.: 19 May 2015

Revised: 26 September 2015 – Accepted: 2 October 2015 – Published: 12 October 2015

Abstract. We use an eddy-resolving, regional ocean biogeochemical model to investigate the main variables and processes responsible for the climatological spatio-temporal variability of pCO₂ and the air-sea CO₂ fluxes in the southwestern Atlantic Ocean. Overall, the region acts as a sink of atmospheric CO₂ south of 30° S, and is close to equilibrium with the atmospheric CO₂ to the north. On the shelves, the ocean acts as a weak source of CO₂, except for the mid/outer shelves of Patagonia, which act as sinks. In contrast, the inner shelves and the low latitude open ocean of the southwestern Atlantic represent source regions. Observed nearshore-to-offshore and meridional pCO₂ gradients are well represented by our simulation. A sensitivity analysis shows the importance of the counteracting effects of temperature and dissolved inorganic carbon (DIC) in controlling the seasonal variability of pCO₂. Biological production and solubility are the main processes regulating pCO₂, with biological production being particularly important on the shelves. The role of mixing/stratification in modulating DIC, and therefore surface pCO₂, is shown in a vertical profile at the location of the Ocean Observatories Initiative (OOI) site in the Argentine Basin (42° S, 42° W).

1 Introduction

Shelf regions are amongst the most biogeochemically dynamical zones of the marine biosphere (Walsh, 1991; Bauer et al., 2013). Even though they comprise only 7–10 % of the global ocean area (Laruelle et al., 2013), continental shelves could contribute to approximately 10–15 % of the ocean primary production and 40 % of the ocean's carbon sequestration through particulate organic carbon (Muller-Karger et al., 2005). Global discussions about the role of continental margins as a sink of atmospheric CO₂ gained momentum after Tsunogai et al. (1999) suggested that these shelf regions take up as much as 1 Pg C yr⁻¹ of atmospheric CO₂. Recent estimates range from 0.2 Pg C yr⁻¹ (Laruelle et al., 2013) to roughly 0.6 Pg C yr⁻¹ (Yool and Fasham, 2001), somewhat more modest than initially thought (Gruber, 2015), but still relevant to the global ocean sink estimated around 2.3 Pg C yr⁻¹ (Ciais et al., 2014).

Continental shelves tend to act as a sink of carbon at high and medium latitudes (30–90°), and as a weak source at low latitudes (0–30°) (Chen et al., 2013; Hofmann et al., 2011; Bauer et al., 2013; Laruelle et al., 2014), i.e., they tend to follow similar meridional trends as the open ocean CO₂ fluxes (Landschützer et al., 2014; Takahashi et al., 2009).

However, continental shelves present a higher spatio-temporal variability of air-sea CO₂ fluxes than the adjacent

open ocean, with the inner shelf and near coastal regions generally acting as a source of CO_2 to the atmosphere, while the mid/outer shelf and the continental slope generally act as sinks (Cai, 2003). This pattern can be explained by the increased primary production and decreased terrestrial supply towards the outer shelf (Walsh, 1991). Seasonality of the upper ocean (e.g. mixing and stratification) may also be important to the air-sea exchange of carbon. For example, the United States southeast continental shelf acts as a sink of CO_2 in the winter and as a source in the summer (Wang et al., 2005).

In the southwestern Atlantic Ocean, the shelf region presents distinct features. To the south, the Patagonian shelf is one of the world's largest shelves with an area close to 10^6 km^2 , broadening to more than 800 km from the coastline (Bianchi et al., 2009). To the north, the Brazilian shelf narrows to around 100–200 km from the coastline. This region is one of the most energetic regions of the world's ocean with the confluence of the warm southward-flowing Brazil Current (BC) and the cold Malvinas Current (MC) flowing northward (Piola and Matano, 2001). The extension of the confluence roughly divides the subtropical and subantarctic oceanic gyres in the South Atlantic and might be a hotspot for shelf-open ocean exchange (Guerrero et al., 2014).

In the open-ocean, the South Atlantic is thought to absorb between $0.3\text{--}0.6 \text{ Pg C yr}^{-1}$ south of 30° S , while acting as a source to the atmosphere north of 30° S (Takahashi et al., 2002). Aside from global open-ocean estimates, only a few local studies were conducted on the continental shelves in this region. The Patagonia shelf was characterized as a source of CO_2 to the atmosphere on the inner shelf, and as a sink in the mid-outer shelf (Bianchi et al., 2009). The southeast Brazilian shelf and continental slope were characterized as sources of CO_2 to the atmosphere during all seasons (Ito et al., 2005). Such regions are often neglected, or poorly resolved, on relatively coarse global modeling assessments, although they may contribute up to 0.2 Pg C yr^{-1} of global ocean CO_2 uptake (Laruelle et al., 2014).

Regional marine biogeochemical models have been used to assess the ocean carbonate system and CO_2 fluxes, including the continental margins. For example, along the US east coast, the seasonality of $p\text{CO}_2$ was found to be controlled mainly by changes in the solubility of CO_2 and biological processes (Fennel and Wilkin, 2009). Along the California coast, biological production, solubility and physical transport (e.g. circulation) were found to be the most influential processes on $p\text{CO}_2$ variability, both spatially and temporally (Turi et al., 2014).

In this study we use a regional marine biogeochemical model coupled to a hydrodynamic model to investigate the parameters and processes regulating the variability of ocean surface $p\text{CO}_2$ in the southwestern Atlantic Ocean. Our model domain includes the location of the global node mooring that is soon to be deployed as part of the

Table 1. Statistical indicators of model skill for surface ocean $p\text{CO}_2$ in the three areas (A1, A2 and A3 – Fig. 4). The indicators are the following: ME (Model Efficiency); CF (Cost Function) and PB (Percentage of Bias). Additionally, showing total bias (μatm), correlation and total number of observations (N) available on each area. Bold values indicate “good/reasonable” model skill.

Area	ME	CF	PB	Bias	Correlation	N
A1	0.23	0.52	2.88	10.26	0.80	77
A2	−0.18	0.61	4.23	15.0	−0.34	60
A3	−4.70	1.83	11.59	40.4	−0.13	40

Ocean Observatories Initiative (OOI) at 42° S , 42° W (www.oceanobservatories.org).

We compare modeled surface $p\text{CO}_2$ distribution with observations and use the results to investigate the relative importance of the parameters (DIC, temperature, alkalinity and salinity) and processes (biological production, air-sea CO_2 flux, CO_2 solubility and physical transport) in controlling surface $p\text{CO}_2$ distribution and variability on the continental shelf and open ocean in the southwestern Atlantic Ocean.

2 Materials and methods

2.1 Model

The physical model used in this study is the Regional Ocean Modeling System (ROMS) (Shchepetkin and McWilliams, 2005). Our model domain spans from 15 to 55° S , and from 70 to 35° W , i.e., covering the southwestern Atlantic from its subtropical to subantarctic latitudes and from the continental shelf all the way out to the open ocean. The horizontal grid resolution is 9 km, with 30 vertical levels with increasing resolution towards the surface.

The biogeochemical model is an NPZD type, including the following state variables: phytoplankton, zooplankton, nitrate, ammonium, small and large detritus, and a dynamic chlorophyll-to-carbon ratio for the phytoplankton (Gruber et al., 2006). A carbon component is also coupled to the model, with the addition of calcium carbonate, DIC and alkalinity to the system of state variables (Gruber et al., 2011; Hauri et al., 2013; Turi et al., 2014). Parameters and values used in the biogeochemical model are listed in Table 1 of Gruber et al. (2006). The CaCO_3 cycle was parametrized as in Hauri et al. (2013). Phytoplankton types as parametrized in the model correspond to the microplankton with large nutrient requirements and relatively fast growth rates (Gruber et al., 2006). Since our domain encompasses several ecological provinces (Gonzalez-Silvera et al., 2004), we may not represent all regions equally well with only one phytoplankton functional type.

The initial and boundary conditions used for the physical variables were obtained from a climatology of the Simple Ocean Data Assimilation (SODA) (Carton and Giese,

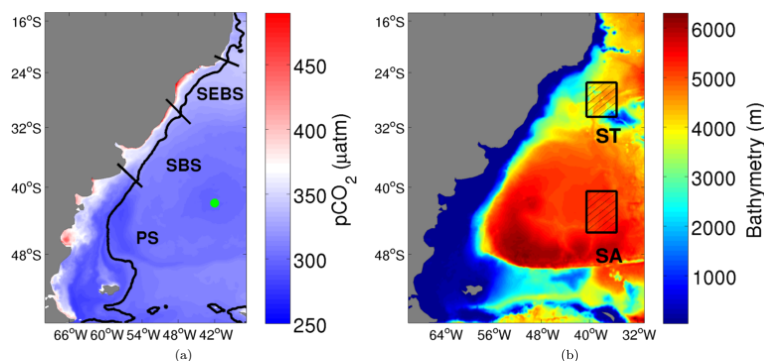


Figure 1. Areas utilized for the temporal analysis, (a) shows the three continental shelves (SEBS, SBS and PS) analyzed in a map with annual mean ocean surface $p\text{CO}_2$. The green circle represents the location of the vertical profile at the OOI site. (b) shows the two oceanic regions (ST and SA) in a map with bathymetry.

2008), and for the biogeochemical variables from a Community Earth System Model (CESM) climatological model product (Moore et al., 2013). The model is forced at the surface with climatological winds from QuikSCAT (Risien and Chelton, 2008) and heat and freshwater surface fluxes from the Comprehensive Ocean-Atmosphere Data Set (COADS) (Da Silva et al., 1994). We used a fixed atmospheric $p\text{CO}_2$ of $370 \mu\text{atm}$ without CO_2 incrementation throughout the years and without seasonal variations. We ran the model for 8 years and used a climatology from years 5 through 8 in our analyses.

Even though processes such as river runoff and tides are locally relevant (i.e., La Plata River, and Patagonia shelf), we are not considering them in the present study (see conclusions section). The low salinity waters from the La Plata river are included in the climatological forcing from COADS which are “nudged” into the model. These shortcomings may affect the results in some regions, but it is unlikely that they will affect the overall $p\text{CO}_2$ results in the wider domain.

2.2 Analysis

Ocean surface $p\text{CO}_2$ is the most important variable determining the air-sea CO_2 flux. This is because the variability of ocean $p\text{CO}_2$ is much greater than that of atmospheric $p\text{CO}_2$, and the impact of variations in the gas transfer coefficient are usually several times smaller than those of ocean surface $p\text{CO}_2$ (Takahashi et al., 2002). Seawater $p\text{CO}_2$ is regulated by the concentration of dissolved inorganic carbon (DIC), alkalinity (ALK), temperature (T) and salinity (S). While T and S are controlled solely by physical factors, DIC and ALK are affected both by biological production and physical transport. DIC concentration is also affected by air-sea CO_2 fluxes (Sarmiento and Gruber, 2006).

In our model, ocean surface $p\text{CO}_2$ is calculated through a full model implementation of the seawater inorganic carbon system, i.e., as a function of the state variables T , S , DIC, and ALK, with the dissociation constants k_1 and k_2 from Millero

(1995). In order to assess the impact of different parameters on $p\text{CO}_2$ variability, we decompose $p\text{CO}_2$ with respect to T , S , DIC and ALK, following the approach of Lovenduski et al. (2007); Doney et al. (2009); Turi et al. (2014) and Signorini et al. (2013),

$$\Delta p\text{CO}_2 = \frac{\partial p\text{CO}_2}{\partial \text{DIC}} \Delta \text{DIC}^s + \frac{\partial p\text{CO}_2}{\partial \text{ALK}} \Delta \text{ALK}^s + \frac{\partial p\text{CO}_2}{\partial T} \Delta T + \frac{\partial p\text{CO}_2}{\partial \text{FW}} \Delta \text{FW}, \quad (1)$$

where the Δ 's are anomalies, either spatial or temporal, relative to a domain or an annual mean, respectively. DIC^s and ALK^s are the variable concentrations normalized to a domain-averaged surface salinity of 34.66, therefore the effects of dilution on DIC and ALK through freshwater input are not included in DIC^s and ALK^s . The dilution effect is considered instead in the freshwater component (FW) that includes the effects of precipitation and evaporation on DIC and ALK concentrations.

The partial derivatives were calculated following Doney et al. (2009). $p\text{CO}_2$ was recalculated four times adding a small perturbation to the spatial, or temporal, domain average for each variable (T , S , DIC, ALK) while maintaining the other three variables fixed to the domain-averaged surface values. The perturbation applied here was 0.1 % of the domain mean.

In order to investigate the parameters and processes controlling $p\text{CO}_2$ on the continental margin, we limited our temporal analysis to three regions with depths shallower than 1000 m: the Southeast Brazilian Shelf (SEBS) in the northern part of the domain, the South Brazilian Shelf (SBS) in the middle of the domain that encompasses the Uruguayan Shelf, and the Patagonia Shelf (PS) to the south of the domain (Fig. 1a). We also selected two open ocean regions for comparison with the continental shelves: a subtropical (ST) and a subantarctic (SA) region (Fig. 1b). In each of these regions, we estimated the monthly contribution of each parameter to the modeled $p\text{CO}_2$ variability by spatially averaging

the parameters within each region, and using the temporal anomalies (subtracting the annual mean) on Eq. (1). For the spatial analysis, we used the whole study area and then calculated in each grid cell the spatial anomalies (subtracting the domain mean of that grid cell), finally applying it to Eq. (1).

In order to identify the main processes responsible for the variability of surface $p\text{CO}_2$, we used a progressive series of sensitivity experiments as in Turi et al. (2014), focusing on the processes of biological production, CO_2 solubility, air-sea CO_2 fluxes, and physical transport. To quantify these processes, we made three additional model runs, progressively excluding each process. In the first experiment (E1), we set the CO_2 gas exchange flux coefficient between the atmosphere and the ocean to zero, inhibiting gas exchange in the surface layer. In the second experiment (E2), we started from E1 and also turned off the photosynthetically available radiation (PAR), preventing phytoplankton growth. Finally, in experiment E3, the CO_2 solubility was set to a constant value, calculated with the domain-averaged surface salinity and temperature of 34.66 and 12.33 °C, respectively, while maintaining the changes of E1 and E2. The control run minus E1 represents the impact of gas exchange between ocean and atmosphere, E1 minus E2 represents the impact of biology, E2 minus E3 represents the impact of variable solubility. The last experiment (E3), in which there is no air-sea flux, no biology and constant solubility represents the impact of physical transport (Turi et al., 2014).

Given the short model integration times, the vertical gradients in the E3 simulation have not come in to steady-state with the processes. So our physical transport is working on the vertical DIC gradients established by the biological pump. Since the lateral boundary conditions are the same for all experiments, these simulations are therefore only approximations of the impact of each process on $p\text{CO}_2$. Furthermore, this separation assumes a linear additionality of each process, which is clearly a strong simplification given the non-linear nature of the inorganic carbonate system (Sarmiento and Gruber, 2006). The same spatial and temporal analysis described for the variables (ALK, DIC, T and FW) was also applied for the processes experiments (air-sea CO_2 flux, biology, CO_2 solubility, physical transport).

3 Model evaluation and validation

Model results were evaluated against data from the Surface Ocean CO_2 Atlas (SOCAT) version 2 (Bakker et al., 2013). SOCAT $f\text{CO}_2$ observations were converted into $p\text{CO}_2$ using the set of equations from Körtzinger (1999) and then compared with modeled $p\text{CO}_2$ to assess the overall skill of the model. Due to the paucity of in situ observations, particularly on the continental shelves, we used monthly climatologies for the comparison. The seasonal model evaluation was made over the whole domain (Fig. 1). On the Patagonia Shelf, data from the Argentinian cruises ARGAU and GEF3 were used for a more focused comparison of the model results (Bianchi

et al., 2009). For the Brazilian continental shelves no data were found for local comparisons.

Overall, our model simulates reasonably well the seasonality of ocean surface $p\text{CO}_2$, with the latitudinal and cross-shelf gradients represented during all seasons (Fig. 2). Since our simulation has a fixed atmospheric $p\text{CO}_2$ of 370 μatm , this value separates the source from the sink regions. In the northernmost oceanic region, between 16 and 30° S, the observations show $p\text{CO}_2$ close to 370–380 μatm . Therefore this region acts as a weak source of CO_2 to the atmosphere. This tendency is well captured by the model, particularly during summer and autumn. From 30 to 55° S, the whole offshore region acts as a CO_2 sink, with $p\text{CO}_2$ ranging from 250 to 350 μatm during all seasons in the model results. The observations show the same pattern down to 50° S. However in the southernmost region the observed $p\text{CO}_2$ rises to values close to 400 μatm . On the Southeast Brazilian Shelf, there were no data for model evaluation, but the overall behavior of $p\text{CO}_2$ agrees with previous results from Ito et al. (2005), who suggested that the continental shelf in this region acts as a source to the atmosphere across both inner and outer shelves during all seasons. The southernmost and northernmost regions are where our model has the largest biases, underestimating the ocean surface $p\text{CO}_2$. These biases could be due to a variety of reasons, including the high variability of the Antarctic Circumpolar Current and/or proximity to the model boundary with potential biases in the lateral boundary conditions used to force the model.

On the Patagonia Shelf the model was evaluated using in situ observations from Bianchi et al. (2009) during the years 2000 to 2006 (Fig. 3). The model agrees very well with the seasonality of the observations of this shelf region, in particular the high $p\text{CO}_2$ values along the inner shelf, which make these regions a source of CO_2 during all seasons, but more intense during autumn/winter (Fig. 3b, c, f, g). In the mid-outer shelf the ocean generally acts as a sink, while to the north the ocean is in equilibrium with the atmosphere particularly during winter.

The monthly analysis was restricted to three offshore areas (A1, A2 and A3 in Fig. 4a). We compared the spatial monthly mean modeled surface $p\text{CO}_2$ with the monthly average of the SOCAT $p\text{CO}_2$ data available in each area. Within these areas, we applied the following statistical indicators used in Dabrowski et al. (2014) in order to quantitatively assess model skill: model efficiency $\text{ME} = 1 - (\Sigma(O - M)^2) / (\Sigma(O - \bar{O})^2)$ (Nash and Sutcliffe, 1970), cost function $\text{CF} = (\Sigma |M - O|) / (n\sigma_o)$ (Ospar et al., 1998) and percentage of bias $\text{PB} = |\Sigma(O - M)| / \Sigma O$ (Allen et al., 2007), where M stands for modeled $p\text{CO}_2$ and O for observations from SOCAT database, n is the number of observations and σ_o is the standard deviation of all observations. These statistics are indicators of the model's performance and provide complementary information of the model skill. ME relates model error with observational variability, CF is the ratio of mean absolute error to standard deviation

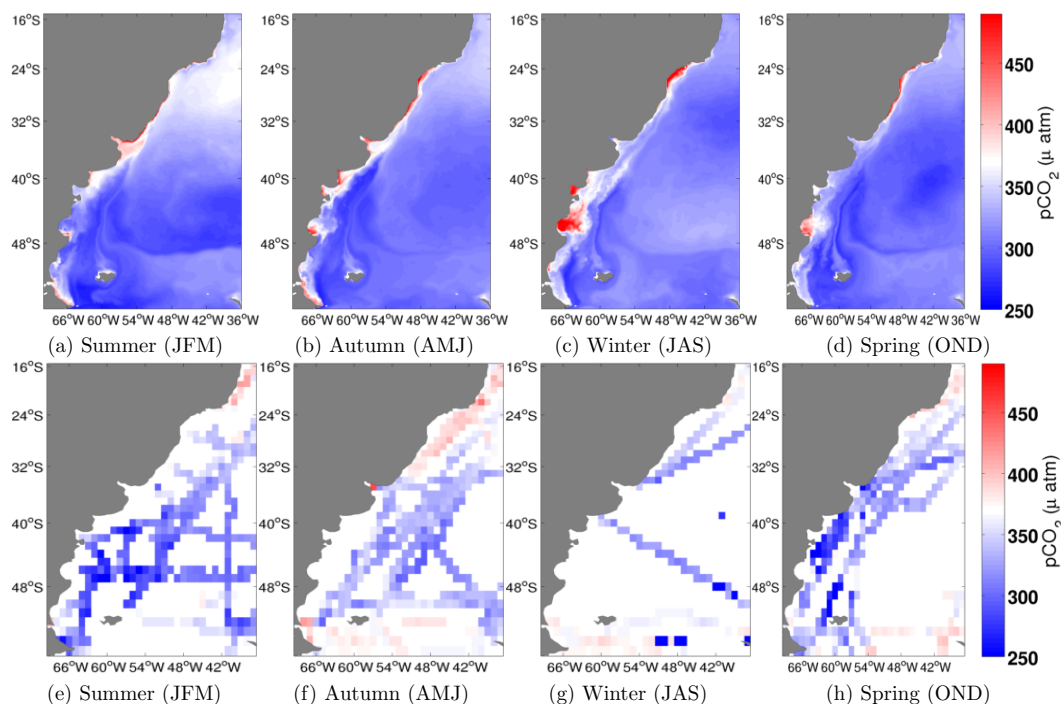


Figure 2. Seasonal climatology of modeled ocean surface $p\text{CO}_2$ (upper row) and observations of $p\text{CO}_2$ from the SOCAT database (lower row). The white separation between red and blue is set to $370 \mu\text{atm}$ which is the atmospheric $p\text{CO}_2$ used in this study. Blue represents a sink of atmospheric CO_2 and red a source.

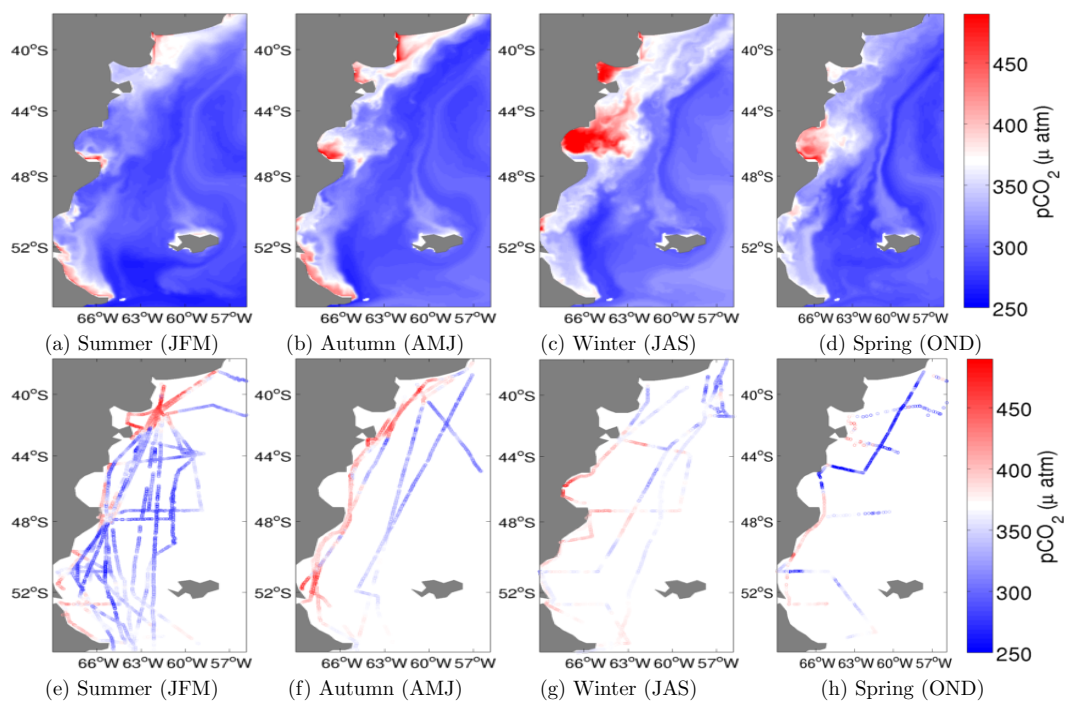


Figure 3. Model evaluation on the Patagonia Shelf (PS) (zoom in from model domain in Fig. 2a). Seasonal climatology of modeled ocean surface $p\text{CO}_2$ (upper row) and $p\text{CO}_2$ observations from ARGAU and GEF3 cruises (lower row) (Bianchi et al., 2009). The white separation between red and blue is set to $370 \mu\text{atm}$ which is the atmospheric $p\text{CO}_2$ used in this study. Blue represents a sink of atmospheric CO_2 and red a source.

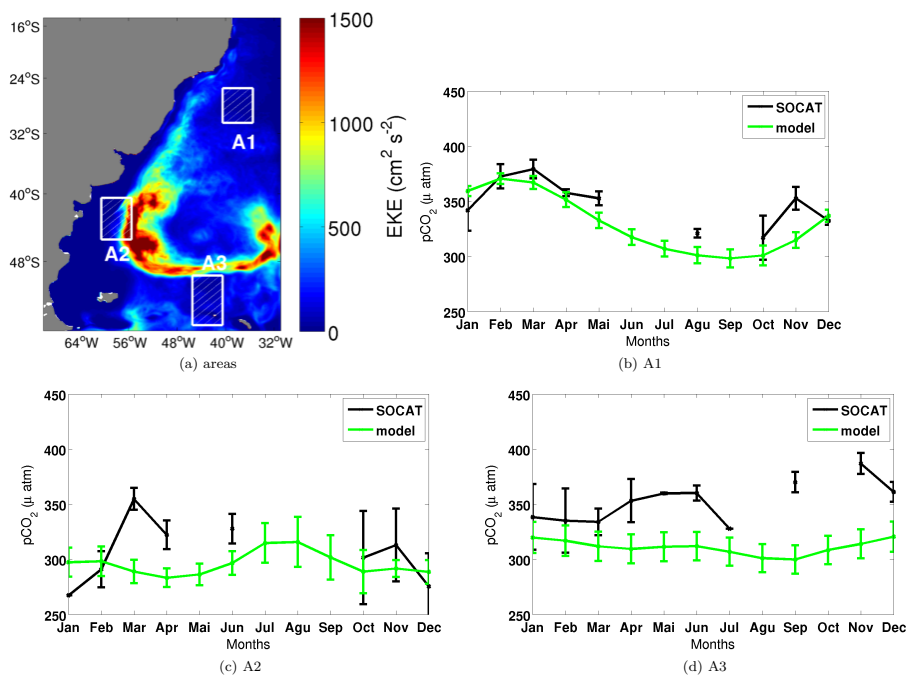


Figure 4. Location of the three areas used for the monthly comparison with SOCAT database (a) in a map with annual mean eddy kinetic energy. In panels (b), (c) and (d), green lines are the modeled monthly mean $p\text{CO}_2$ and black lines are the monthly mean $p\text{CO}_2$ from SOCAT. Error bars are two standard deviations.

of observations, and PB is the bias normalized by the observations (Dabrowski et al., 2014; Stow et al., 2009). Basically if $\text{ME} > 0.5$, $\text{CF} < 1$ and $\text{PB} < 20$, this indicates that the model is “good/reasonable” when comparing to observations. If $\text{ME} < 0.2$, $\text{CF} > 3$ and $\text{PB} > 40$ the model is classified as “poor/bad”.

Modeled $p\text{CO}_2$ results for A1 agree very well with the observations, representing the $p\text{CO}_2$ evolution throughout the year with maximum values in summer (Fig. 4b). All statistical indicators characterized the model with a good/reasonable skill in A1 (Table 1).

A2 is the region with the largest $p\text{CO}_2$ standard deviation from both model and observations (Fig. 4c). This region is near the confluence between the warm Brazil Current and the cold Malvinas Current, generating one of the most energetic regions of the world’s oceans. Moreover, this region comprises the shelfbreak front, with differences in stratification, local dynamics and salinity between shelf waters and Malvinas current waters (Fig. 4a). Consequently, ME was estimated as poor/bad in this region, probably due to the high $p\text{CO}_2$ data variability. But CF and PB were both rated as “good/reasonable” (Table 1).

In A3 the model consistently underestimated $p\text{CO}_2$ (Fig. 4d). This bias is seen in the seasonal comparison and in the monthly analysis, where summer is the only season for which modeled $p\text{CO}_2$ is within the standard deviation of the observations. ME was estimated as poor/bad in A3, but PB and CF rated our model as reasonable and good, respectively.

(Table 1). Both A2 and A3 regions are close to an area of elevated eddy kinetic energy (Fig. 4a), which could explain the large standard deviation and biases in these regions.

The Taylor diagram is consistent with the model efficiency (ME) estimate, showing good/reasonable results in A1, with a correlation of 0.8, and poor results in A2 and A3, with negative correlations (Fig. 5). Only in A1 the correlation was found to be statistically significant. Aside from greater $p\text{CO}_2$ variability in these regions, the poor results found in A2 and A3 could also be due to the paucity of the observational data both in space and time.

Furthermore, in order to validate the baseline of our model, seasonal climatologies of modeled sea-surface temperature and chlorophyll *a* were compared with climatologies from AVHRR and MODIS-aqua, respectively. Results and a detailed discussion of this validation are shown in the Appendix.

In conclusion, our model reproduces the most important north-south and inner-outer shelf gradients seen in the $p\text{CO}_2$ observations. While there is clearly room for improvement, we deem this level of agreement as sufficient for proceeding to the analysis of the processes and parameters affecting $p\text{CO}_2$ variability in this region.

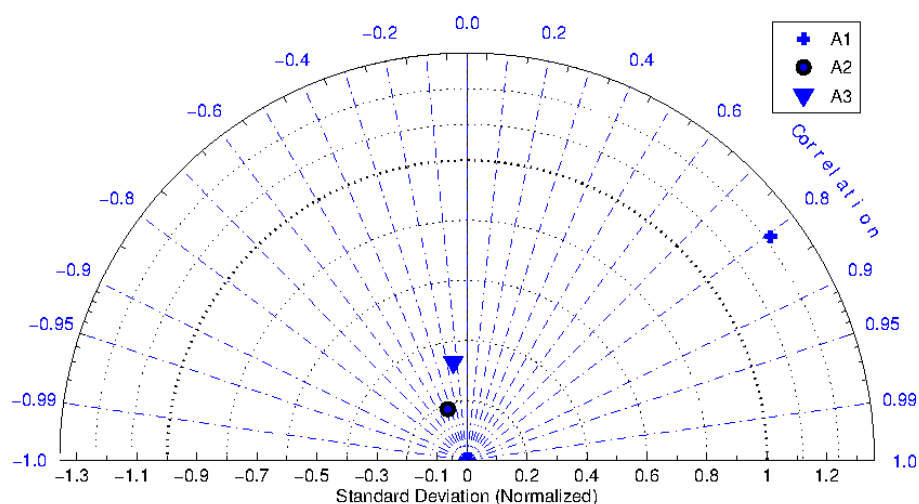


Figure 5. Taylor Diagram showing the three areas used for comparison with SOCAT observational data. A1 is the only area with statistically significant correlation.

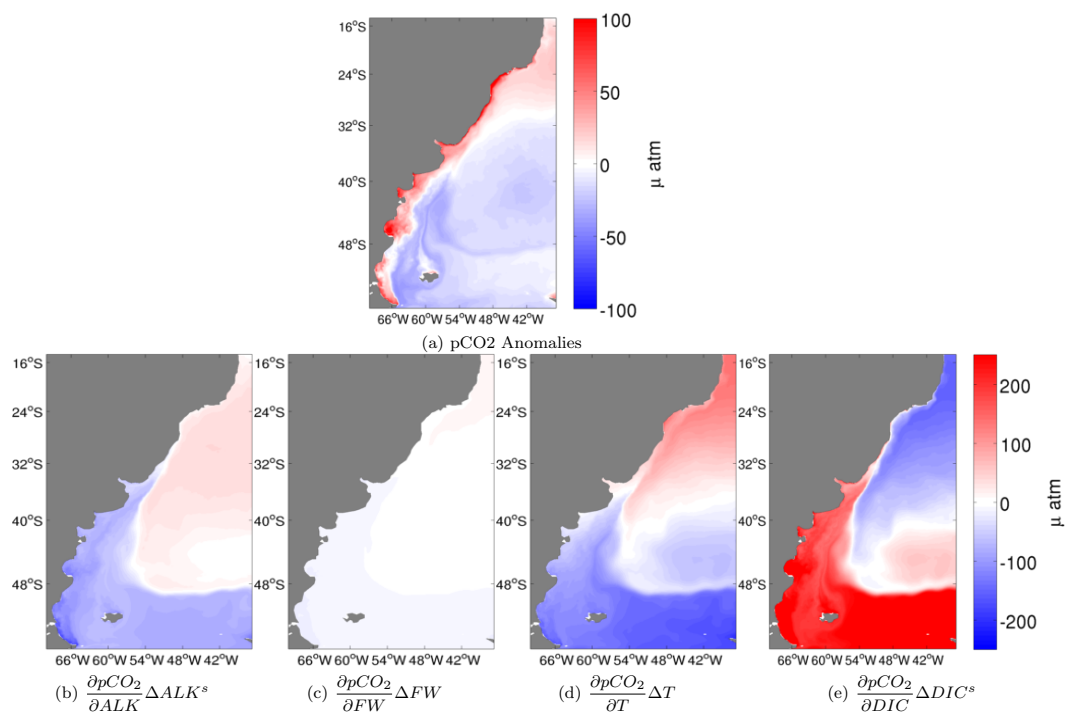


Figure 6. *p*CO₂ spatial anomalies – difference between annual mean and domain mean (a) and the contribution of the main drivers: ALK^s (b), FW (c), *T* (d) and DIC^s (e). Computed using spatial anomalies for Δ .

4 Results and Discussion

4.1 *p*CO₂ drivers – spatial analysis

Modeled *p*CO₂ spatial anomalies relative to the domain average are shown in Fig. 6a, with positive anomalies prevailing on the Brazilian continental shelves, inner-mid Patagonia Shelf and North of 32° S, while the negative anomalies are

found in the open ocean south of 32° S and in the mid-outer Patagonia Shelf. DIC^s has the highest impact on the spatial variations, being counteracted by ALK^s and *T* (Fig. 6). In contrast, the fresh water flux has a minor influence on the spatial anomalies of *p*CO₂, agreeing with Turi et al. (2014) and Doney et al. (2009). Despite its smaller role, the influence of ALK^s on *p*CO₂ anomalies was higher (−100 to 100 μatm) than those found in previous studies in other re-

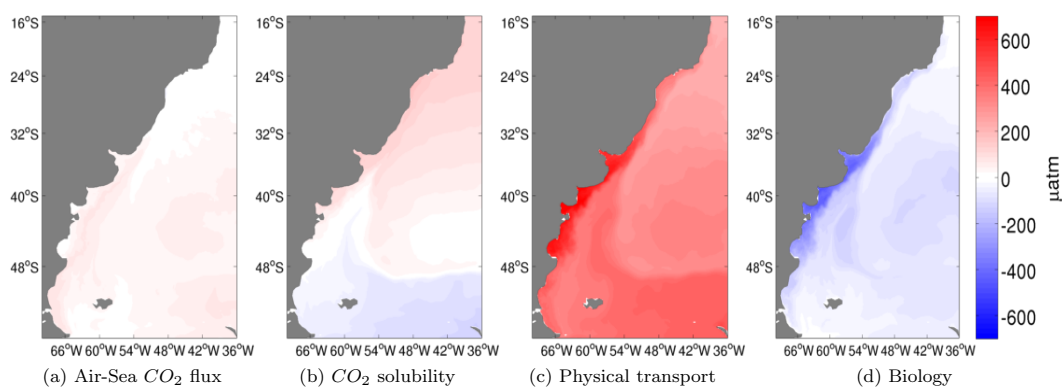


Figure 7. Processes driving the annual mean surface $p\text{CO}_2$. Contribution of Air-sea flux of CO_2 [Control–E1] (a), CO_2 solubility [E2–E3] (b), physical transport [E3] (c) and biological production [E1–E2] (d).

gions (Lovenduski et al., 2007; Turi et al., 2014). The higher contribution of both DIC^s and ALK^s to the spatial variations in $p\text{CO}_2$ could be explained by the more heterogeneous domain that encompasses several distinct surface water masses and frontal zones. Also, the elevated contribution of ALK^s could be due to our relatively high CaCO_3 to biological production ratio of 0.07.

The changes in the state variables affecting $p\text{CO}_2$ are ultimately being driven by physical and biogeochemical processes. We investigate the role of each of these processes in controlling the changes in surface $p\text{CO}_2$ from our sensitivity experiments (E1, E2, E3). The most important processes affecting the spatial distribution of $p\text{CO}_2$ are biological production (E1–E2) and physical transport (E3) (Fig. 7). When physical transport (vertical and horizontal) is the only process altering $p\text{CO}_2$, we observe an increase in $p\text{CO}_2$ of up to $800 \mu\text{atm}$ on the continental shelves, due to the upwelling and vertical mixing of DIC -rich subsurface waters. At the same time, the effect of biological production on the uptake of DIC and changes in ALK due to nitrate uptake and production/dissolution of CaCO_3 accounts for a decrease of up to $-600 \mu\text{atm}$ on the continental shelves. Solubility effects (E2–E3) are responsible for a decrease in $p\text{CO}_2$ south of 45°S and an increase in $p\text{CO}_2$ to the north, ranging from -50 to $50 \mu\text{atm}$. Finally, air-sea CO_2 fluxes (Control–E1) have little impact on regulating the ocean surface $p\text{CO}_2$. The effect of both biological production and physical transport is highest on the continental shelves. The balance between these processes also largely control $p\text{CO}_2$ in the open ocean. North of 45°S , biological production is counteracted by physical transport and, to a minor extent, solubility, whereas south of 45°S physical transport is counteracted by biological production and solubility.

The strong effect of biological production on the shelf region is a result of the elevated nutrient supply and high primary production found in these regions, with increasing contribution towards the inner shelves. Physical transport also presents a higher contribution on the continental shelves,

where the mixed layer often spans the entire water column, showing the importance of vertical mixing in bringing DIC as well as nutrients to the surface waters, therefore increasing $p\text{CO}_2$. These results are in agreement with previous studies (c.f. Turi et al. (2014)), showing the importance of the biological net community production and advection of ALK and DIC (physical transport) in controlling ocean surface $p\text{CO}_2$. This suggests a major role of net community production in reducing ocean $p\text{CO}_2$ in the region.

4.2 $p\text{CO}_2$ drivers – temporal analysis

In order to identify the seasonal variability of the contribution of each parameter, we used local grid temporal anomalies over the seasonal cycle (Fig. 8). DIC^s and T are still the most influential parameters, with increasing importance on the continental shelves. The contribution by ALK^s is relevant only on continental shelves south of 32°S , and FW have a minor influence (not shown). It is important to highlight that the magnitude of the signals seen in this analysis is one order of magnitude smaller than the previous spatial analysis. This is likely due to our large and heterogeneous domain, which results in large spatial gradients as compared to the range found over the seasonal cycles.

The contribution of the state variables in each continental shelf region (Fig. 9) shows that these three regions have distinct characteristics, with different contributions from each parameter. In all three regions, DIC^s and T are the most important parameters affecting $p\text{CO}_2$ anomalies, albeit with opposing and seasonally varying contributions. While in summer the T contribution increases $p\text{CO}_2$, that of DIC^s acts to diminish $p\text{CO}_2$. The opposite occurs in winter. The Southeast Brazilian Shelf (SEBS) is the region with the least variability in $p\text{CO}_2$ anomalies, with the contributions of both DIC^s and T in this region ranging from -10 to $10 \mu\text{atm}$.

The South Brazilian Shelf (SBS) is the region with the largest variability in $p\text{CO}_2$ anomalies, with ALK^s having the most prominent impact on $p\text{CO}_2$ as compared to the other

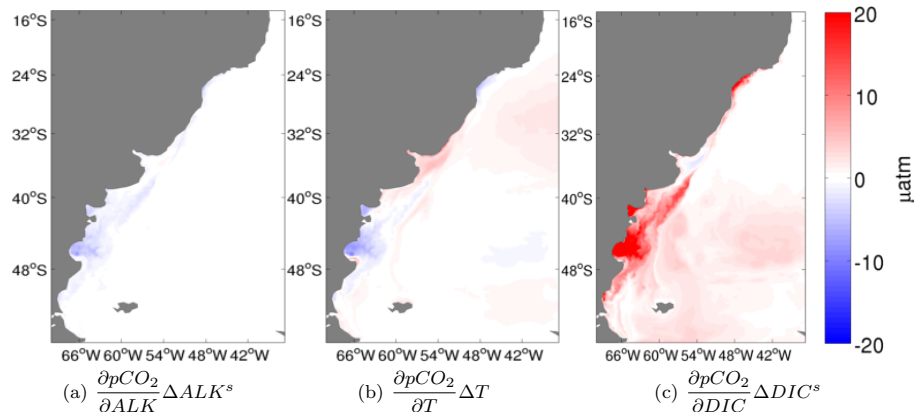


Figure 8. Sensitivity of $p\text{CO}_2$ computed with grid point anomalies in time to local annual means. Annual mean contribution of the main drivers: ALK^s (a), T (b) and DIC^s (c).

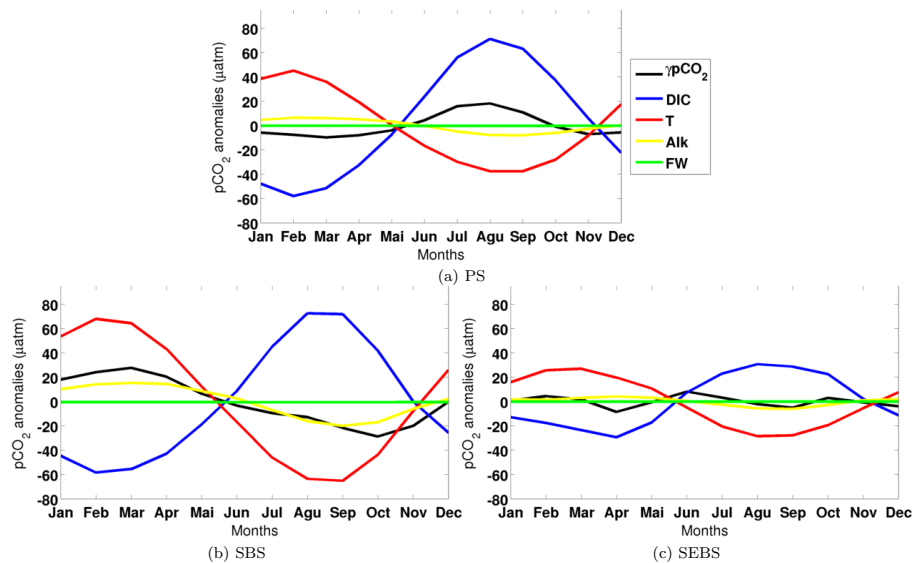


Figure 9. Temporal evolution of $p\text{CO}_2$ anomalies and their drivers in each continental shelf (right hand side of Eq. (1) using temporal anomalies), red line represents the effects of Temperature, blue line the effects of DIC^s , green line FW, and yellow line ALK^s .

regions (up to 15 μatm in spring). DIC^s is the most important parameter in this area, with a contribution of up to 70 μatm , followed by temperature, with a contribution of up to 60 μatm in the winter. On the Patagonia Shelf (PS) and South Brazilian Shelf (SBS), although the contributions by DIC^s and T are large, the tendency of these two terms to cancel each other out results in smaller $p\text{CO}_2$ anomalies. In both SBS and PS, $p\text{CO}_2$ is predominately controlled by T and DIC^s , with small contributions from ALK and FW .

Seasonal warming/cooling largely controls $p\text{CO}_2$ anomalies throughout the continental shelves. This signal is dampened by DIC^s , but also by ALK^s in the case of the South Brazilian Shelf (SBS). This pattern of seasonal variation of the parameters on continental shelves agrees with the results from Signorini et al. (2013) and Turi et al. (2014), although with different absolute values. The pattern of dimin-

ishing variability towards subtropical continental shelves is also shown by Signorini et al. (2013).

This pattern of opposing contributions of T and DIC^s was also found along the North American east coast by Signorini et al. (2013), who attributed winter mixing and the spring-summer biological drawdown as the processes responsible for $p\text{CO}_2$ and DIC variability. In the offshore subtropical region (ST) the $p\text{CO}_2$ anomalies have higher amplitudes than in the adjacent continental shelf (SEBS), and are driven mainly by temperature, with the other variables having minor contributions (Fig. 11). In the offshore southern region (SA), DIC^s controls $p\text{CO}_2$ variability, with T and ALK^s dampening $p\text{CO}_2$ anomalies (Fig. 11), similar to the adjacent shelf (PS).

The analysis of the processes underlying this seasonal variability using our progressive sensitivity simulations

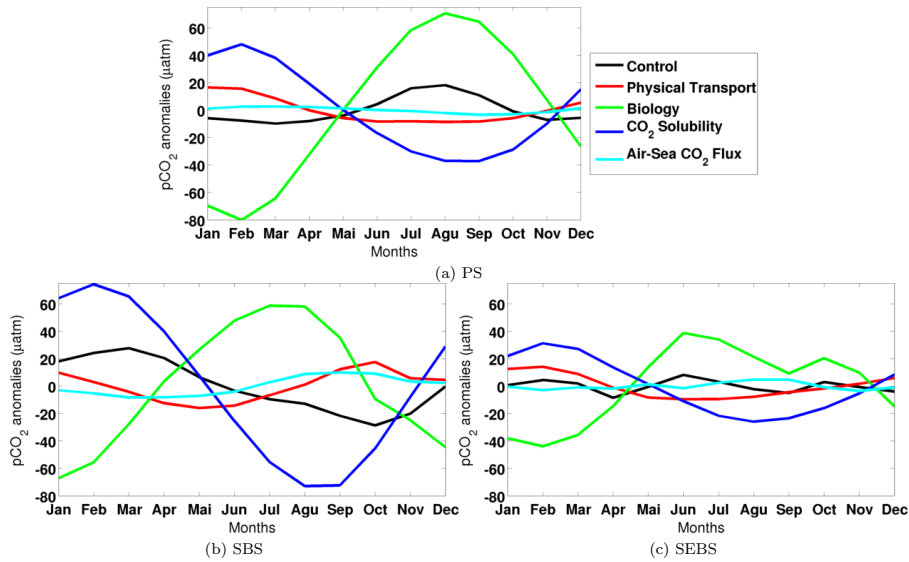


Figure 10. Temporal evolution of the monthly anomalies of each process in regulating *pCO₂* anomalies, green line represents the biological production, red line the physical transport, light blue line the air-sea CO₂ fluxes and dark blue line the CO₂ solubility. Black lines represent the temporal *pCO₂* anomalies.

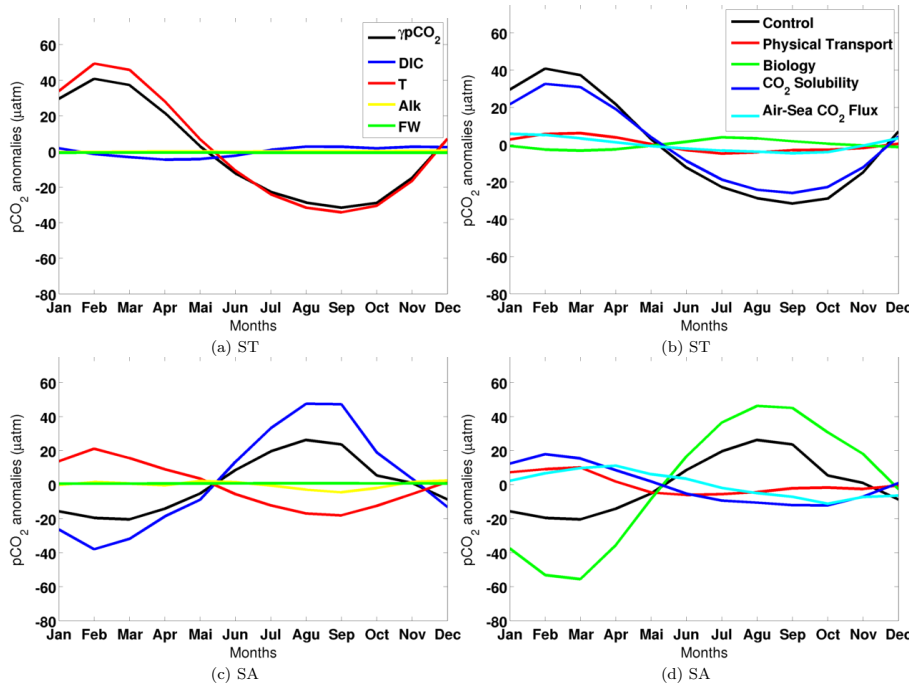


Figure 11. Panels (a) and (b) show the temporal evolution of *pCO₂* anomalies and its drivers in each oceanic regions (ST and SA) (right hand side of Eq. (1) using temporal anomalies), red line represents the effects of *T*, blue line the effects of DIC^S, green line the FW and yellow line ALK^S. Panels (c) and (e) show the temporal evolution of the monthly anomalies of each process in regulating temporal *pCO₂* anomalies, green line represents the biological production, red line the physical transport, light blue line the air-sea CO₂ fluxes and dark blue line the CO₂ solubility. Black lines represent the temporal *pCO₂* anomalies.

shows that on all shelf regions, biological production and CO₂ solubility mostly control *pCO₂* variability (Fig. 10). Physical transport, although weaker than biological produc-

tion, acts to diminish the *pCO₂* variability by counteracting the effects of biology and increasing DIC concentrations. In our case, physical transport controls *pCO₂* spatially, but the

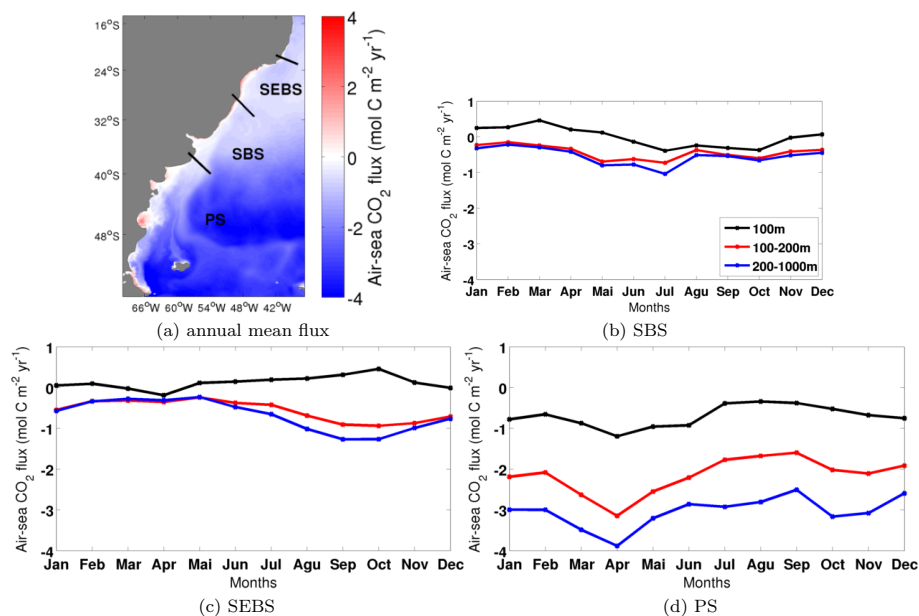


Figure 12. Panel (a) is the annual mean of air-sea CO₂ fluxes. Panels (b), (c) and (d) show the monthly average of surface CO₂ fluxes constrained to bathymetry levels of 100, 200 and 1000 m.

temporal effects of physical transport are much weaker than in Turi et al. (2014) along the California coast. This is probably due to the much stronger upwelling in that region that dampens the effects of biology by bringing DIC rich waters to the surface. Along western boundaries, upwelling is weaker and more localized. Physical transport is therefore more related to processes that modulate vertical mixing and stratification (thereby controlling the seasonal enrichment of surface waters) and horizontal advection due to the presence of two major western boundary currents. Finally, air-sea CO₂ fluxes show only a minor contribution to the $p\text{CO}_2$ anomalies.

In conclusion, on the Patagonia Shelf (PS), the biological production is the most important contributor to $p\text{CO}_2$ variability, with a peak summer contribution of $-80 \mu\text{atm}$ and a maximum in the winter of $70 \mu\text{atm}$. On the South Brazilian Shelf (SBS), solubility is the most influential process (up to $90 \mu\text{atm}$), followed by biological production and physical transport, during all seasons. On the Southeast Brazilian Shelf (SEBS), the pattern is the same as in the SBS, although with a smaller magnitude and variability. Physical transport, although large in absolute contributions in the spatial analysis, has a lower contribution to $p\text{CO}_2$ variability in the temporal analysis.

In the subtropical region, processes that control the temporal variability of $p\text{CO}_2$ on the shelf and offshore are different. In the open ocean (ST) (Fig. 11) $p\text{CO}_2$ is mainly controlled by solubility, with biological production having the least effect on $p\text{CO}_2$. This contrasts with the importance of biology at mid/low latitude continental shelves (SEBS). In the subantarctic region, the processes controlling $p\text{CO}_2$ are similar

for both the offshore region (SA) and the adjacent continental shelf (PS) (Figs. 10 and 11). In this case biological production is the most important process countered mainly by solubility, although with a smaller magnitude in the offshore region.

4.3 Air-sea CO₂ fluxes

On the continental margins, we investigate monthly averaged air-sea CO₂ fluxes on the inner shelf (0–100 m depth), mid-outer shelf (100–200 m depth) and shelf break-slope (200–1000 m depth) (Fig. 12a). As shown in the previous sections, the inner shelves have a potential to act as a source of CO₂, while the mid/outer shelves tend to act as a sink of CO₂. On the Brazilian shelves (SBS and SEBS) the flux density of CO₂ in the inner shelves is around 0 and $0.5 \text{ mol C m}^{-2} \text{ yr}^{-1}$, thus this region acts as a weak source. On the mid/outer shelf a shift towards CO₂ sink occurs, with a flux density of between -1 and $0 \text{ mol C m}^{-2} \text{ yr}^{-1}$ on the Southeast Brazilian shelf (SEBS) (Fig. 12c). On the mid/outer South Brazilian Shelf (SBS) the sink is slightly stronger with an average flux between -1.5 and $-0.5 \text{ mol C m}^{-2} \text{ yr}^{-1}$ (Fig. 12b). The Patagonia Shelf (PS) acts on average as a sink of CO₂, with fluxes larger than on the Brazilian shelves. CO₂ uptake intensifies from the inner Patagonian shelf (-1.0 to $-0.5 \text{ mol C m}^{-2} \text{ yr}^{-1}$) to the outer shelf and continental slope (-2.0 to $-4.0 \text{ mol C m}^{-2} \text{ yr}^{-1}$) (Fig. 12d). Although, overall the PS acts on average as a sink, there are some coastal regions that act as a source of CO₂, in agreement with the observations of Bianchi et al. (2009).

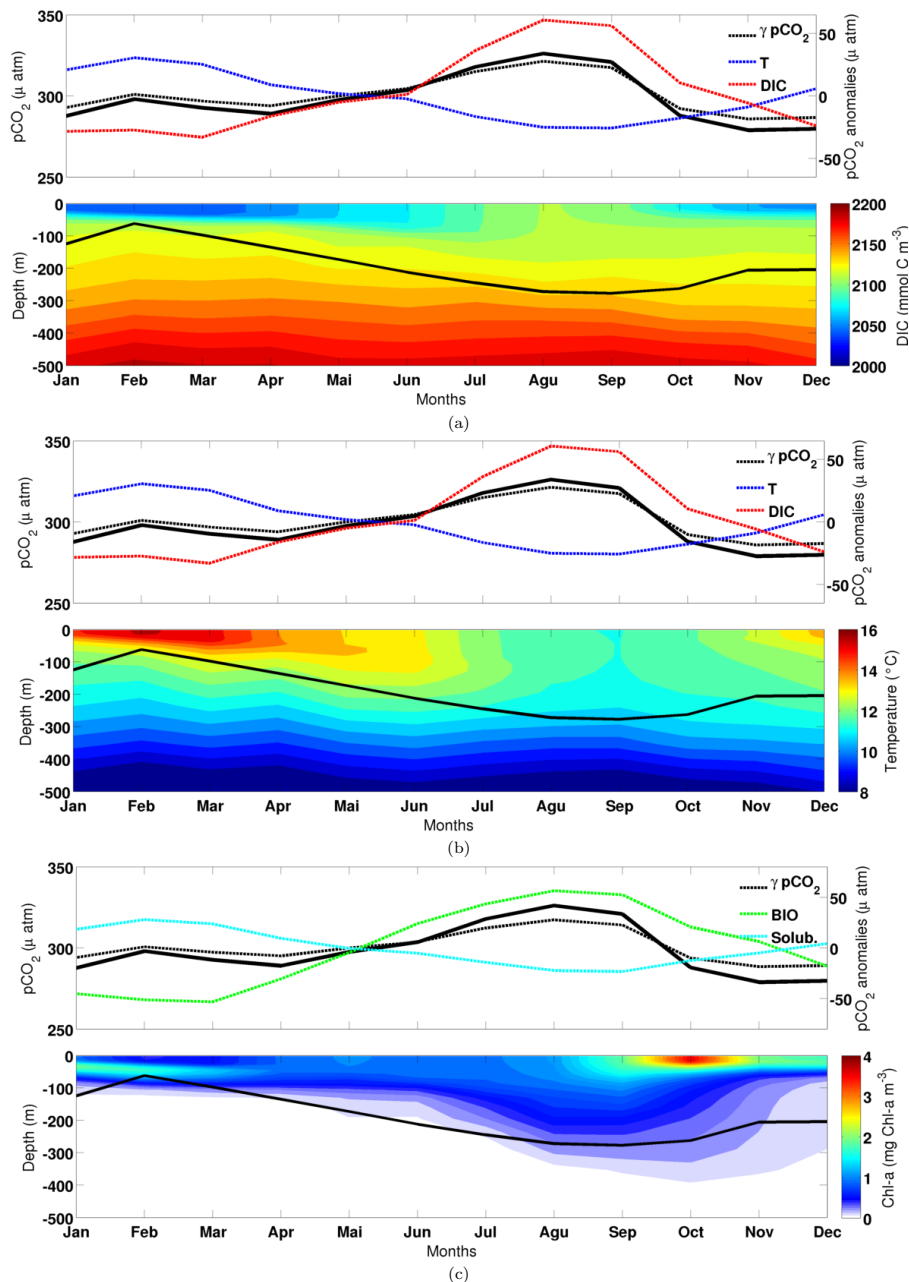


Figure 13. Vertical profile at 42°S , 42°W . Upper panels showing monthly mean surface $p\text{CO}_2$ (solid black line), $p\text{CO}_2$ anomalies (dashed black line) and the contribution from T and DIC^s (red and blue dashed lines) and the contribution of biology and solubility (green and cyan dashed lines). Lower panels showing vertical profiles of DIC (a), T (b), and chlorophyll a (c), black line represents the mixed layer depth.

Annual mean modeled air-sea CO_2 fluxes agreed reasonably well with global climatologies in the oceanic regions (not shown) (Takahashi et al., 2002; Landschützer et al., 2014). South of 30°S , the open ocean acts on average as a sink of atmospheric CO_2 , uptaking up to $4\text{ mol C m}^{-2}\text{ yr}^{-1}$. North of 30°S , the open ocean is on average in equilibrium with the atmosphere (Fig. 12a). On the continental margins, our annual mean air-sea CO_2 fluxes compare well with the global estimate from Laruelle et al. (2014),

with the Patagonia Shelf acting as a CO_2 sink (-1.0 to $-3.0\text{ mol C m}^{-2}\text{ yr}^{-1}$) and the Brazilian shelves as weak sources (0 to $1\text{ mol C m}^{-2}\text{ yr}^{-1}$). Nevertheless, we found variability in these areas, with regions on the inner Patagonia Shelf acting as a source or in equilibrium with the atmosphere (0 to $2.0\text{ mol C m}^{-2}\text{ yr}^{-1}$), and regions on the outer Brazilian shelves acting as sinks of CO_2 .

4.4 Vertical structure – case study at Argentine OOI site

Seasonal variations in mixing and stratification control the evolution of the mixed layer depth and consequently the vertical structure of the state variables of the carbonate system. Diapycnal fluxes and uptake of DIC by primary producers are important processes regulating ocean surface $p\text{CO}_2$ (Rippeth et al., 2014). Therefore, surface $p\text{CO}_2$ variability is linked to variations in mixed layer depths.

In order to understand the seasonal evolution of the upper ocean vertical distribution of the state variables in the region and how it affects surface $p\text{CO}_2$, we chose the location of the Ocean Observatory Initiative (OOI) site in the Argentine Basin at 42°S , 42°W (Fig. 1a), as it will soon become a test-bed for the validation of biogeochemical models globally and regionally. We extracted modeled climatological vertical profiles of DIC concentration, temperature and chlorophyll a , and compared with the modeled surface $p\text{CO}_2$ and mixed layer depth (Fig. 13).

During the entire year, this location acts in our model as a sink for atmospheric CO_2 , with modeled surface $p\text{CO}_2$ ranging from 280 to $320\ \mu\text{atm}$. The contribution of DIC^s and T are again driving surface $p\text{CO}_2$ anomalies. In this case DIC^s is controlling the anomalies signal, being modulated by temperature. The main processes affecting $p\text{CO}_2$ in this location is biological production and solubility. Minimum $p\text{CO}_2$ in summer coincides with strong stratification and elevated subsurface biological production, respectively, with the opposing contribution of DIC^s and T leading to $p\text{CO}_2$ anomalies near zero. Maximum $p\text{CO}_2$ occurs when the mixed layer depth deepens, during fall and winter, causing an increase in DIC concentrations in surface waters. This has a larger effect on $p\text{CO}_2$ than the decrease in temperature, resulting in positive $p\text{CO}_2$ anomalies. The excess of DIC is consumed by biological fixation during spring and summer, thus reducing surface $p\text{CO}_2$.

5 Conclusions

In this study, we used climatologies derived from a regional hydrodynamic model coupled to a biogeochemical model to investigate the main parameters and processes that control ocean surface $p\text{CO}_2$ and air-sea CO_2 fluxes in the southwestern Atlantic Ocean. Modeled ocean surface $p\text{CO}_2$ compared well with the available in situ data, reproducing the expected meridional and cross-shelf gradients of $p\text{CO}_2$, with elevated $p\text{CO}_2$ in the inner shelves and at lower latitudes. Our results highlight that the most important variables controlling the spatio-temporal variability of $p\text{CO}_2$ are T and DIC^s . These two variables have opposing effects on $p\text{CO}_2$ and have been shown to be the main drivers of $p\text{CO}_2$ both in global (Sarmiento and Gruber, 2006; Doney et al., 2009) and in other regional studies (Turi et al., 2014; Signorini et al., 2013; Lovenduski et al., 2007). ALK^s is of secondary im-

portance as a spatial regulator of $p\text{CO}_2$, with larger impacts particularly in the South Brazilian Shelf (SBS) and in the southern open ocean region (SA).

The most important processes underlying changes on the state variables and thus on $p\text{CO}_2$ are biological production and CO_2 solubility. Biological production is particularly important on the continental shelves, with higher contribution at high latitudes. In the open ocean, CO_2 solubility is the main process driving $p\text{CO}_2$ variations in the subtropics, while in the subantarctic both CO_2 solubility and biological production are important drivers of $p\text{CO}_2$ variability.

The southwestern Atlantic Ocean acts, on average, as a sink of atmospheric CO_2 south of 30°S , and is close to equilibrium to the north. In the inner continental shelves the ocean acts either as a weak source or is in equilibrium with the atmosphere. To the outer shelf the ocean shifts to a sink of CO_2 . The entire Patagonian shelf acts, on average, as a sink, but there are some particular regions in the inner shelf that acts as a source of CO_2 . The total integrated flux agrees well with Laruelle et al. (2014), particularly on the Brazilian Shelves (SEBS and SBS). In the Patagonia Shelf (PS), we found a slightly stronger sink on the mid/outer Patagonian Shelf (-1.0 to $-3.0\ \text{mol C m}^{-2}\ \text{yr}^{-1}$) and more variability towards the inner shelf.

Our model does not include river inputs of carbon, which are known to be an important factor regulating $p\text{CO}_2$ (Bauer et al., 2013). The lack of tides may adversely affect our model results in the inner shelf of Patagonia, where tidal amplitudes can reach up to 12 m (Kantha, 1995; Saraceno et al., 2010) and tidal fronts are known to impact oceanic $p\text{CO}_2$ (Bianchi et al., 2005). In future regional studies focused on the Patagonia shelf, tides and river run-off should be included.

Modeling studies such as this one depend heavily on in situ observations, the lack of which hampers our ability to properly refine our model. This will certainly be improved by future efforts in data assimilation from vertical profiles of biogeochemical and physical variables collected at the OOI site in the Argentine basin. This study is a first step towards understanding the processes controlling surface $p\text{CO}_2$ in an undersampled, yet highly important, region of the world's ocean.

Appendix A: Model validation (SST and chlorophyll *a*)

Seasonal climatologies of 4 years of modeled sea surface temperature and chlorophyll *a* concentration were compared with climatologies from the sensors AVHRR (1985–2002) and Modis-aqua (2003–2013), respectively (Figs. A1 and A2). Modeled sea surface temperature compared well with AVHRR (Fig. A1) representing both subantarctic and subtropical oceanic regions during all seasons.

Modeled chlorophyll *a* concentration reproduces the general pattern from MODIS-aqua (Fig. A2), with low concentrations in the oceanic regions and higher concentrations on the continental shelves. However, modeled chlorophyll *a* concentrations are overestimated in the open ocean regions ($0.5 \text{ mg Chl } a \text{ m}^{-3}$), especially in the spring season (up to $1 \text{ mg Chl } a \text{ m}^{-3}$). In the coastal regions, we underestimate chlorophyll *a* on the Patagonia Shelf during spring and summer seasons. Expectedly, there was an underestimation in the La Plata region, since we are not modeling the nutrient and organic loads from the river. Finally, on the Brazilian shelf our model overestimates chlorophyll *a*, particularly during summer and spring seasons. These biases may be due to our application of a relatively simple ecosystem model with only one phytoplankton functional type in such a wide region, which encompasses several ecological provinces. Nevertheless, the general pattern is well reproduced in this first effort in modeling the biogeochemistry of the southwestern Atlantic Ocean, and the biases may not significantly compromise our analysis of drivers and processes of $p\text{CO}_2$ variability.

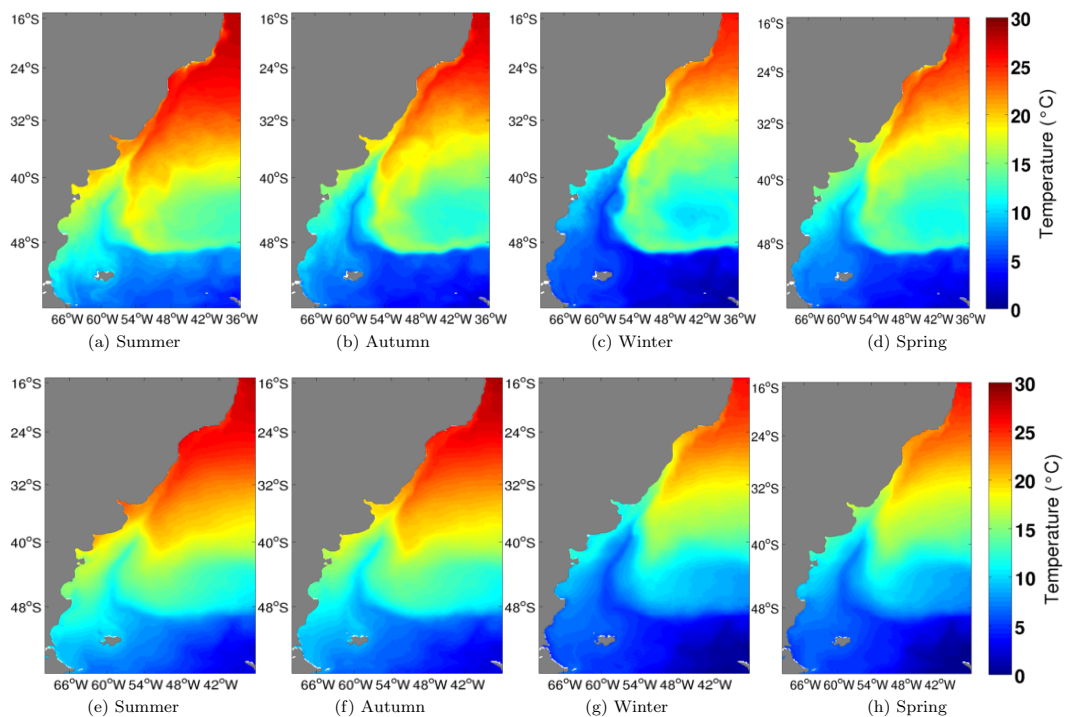


Figure A1. Seasonal climatology of modeled sea surface temperature °C – 4 years average (upper row), and climatology from AVHRR sensor – from 1985 to 2002 (lower row).

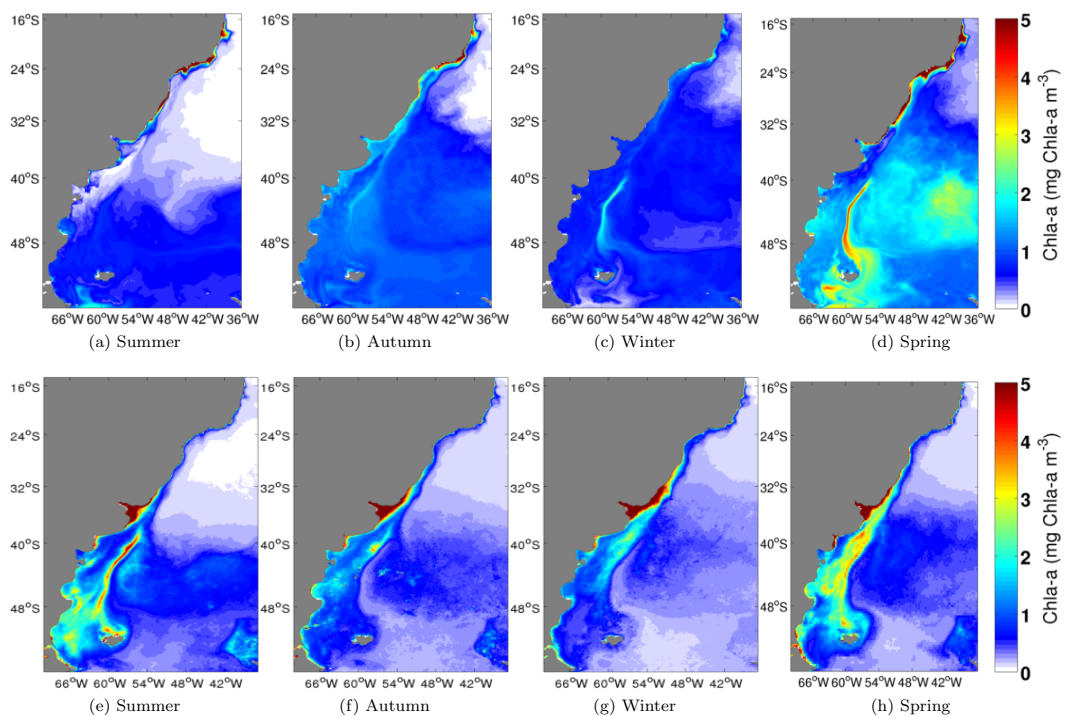


Figure A2. Seasonal climatology of modeled chlorophyll *a* concentration mg Chl *a* m⁻³ – 4 years average (upper row), and climatology from Aqua-Modis sensor – from 2003 to 2013 (lower row).

Acknowledgements. P. H. R. Calil acknowledges support from the Brazilian agencies Conselho Nacional de Desenvolvimento Científico e Tecnológico (CNPq), grants 483112/2012-7 and 307385/2013-2, and the Coordenação de Aperfeiçoamento de Pessoal de Nível Superior (CAPES Process 23038.004299/2014-53). R. Arruda acknowledges support from a CAPES scholarship. S. C. Doney and I. Lima acknowledge support from the National Science Foundation (NSF AGS-1048827). N. Gruber and G. Turi received support from ETH Zurich and from the EU FP7 project CarboChange (264879).

The Surface Ocean CO_2 Atlas (SOCAT) is an international effort, supported by the International Ocean Carbon Coordination Project (IOCCP), the Surface Ocean Lower Atmosphere Study (SOLAS), and the Integrated Marine Biogeochemistry and Ecosystem Research program (IMBER), to deliver a uniformly quality-controlled surface ocean CO_2 database. The many researchers and funding agencies responsible for the collection of data and quality control are thanked for their contributions to SOCAT.

We are greatly indebted with the Ministerio de Defensa de Argentina that supported the project “Balance y variabilidad del flujo mar-aire en el Mar Patagónico” (PIDDEF 47/11). This work was carried out with the aid of a grant from the Inter-American Institute for Global Change Research (IAI) CRN3070 which is supported by the US National Science Foundation (Grant GEO-1128040).

Supported by Global Environmental Facilities (GEF) in the frame of PNUD ARG/02/018-GEF BIRF No. 28385-AR, sub-project B-B46, and by Servicio de Hidrografía Naval. Additional support was provided by the ARGAU Project, Instituto Antártico Argentino, Institut National de Sciences de l’Univers, Processus Biogéochimiques dans l’Océan et Flux, Université Pierre et Marie Curie.

Edited by: C. Klaas

References

- Allen, J., Somerfield, P., and Gilbert, F.: Quantifying uncertainty in high-resolution coupled hydrodynamic-ecosystem models, *J. Marine Syst.*, 64, 3–14, doi:10.1016/j.jmarsys.2006.02.010, 2007.
- Bakker, D. C. E., Pfeil, B., Smith, K. et al.: An update to the Surface Ocean CO_2 Atlas (SOCAT version 2), *Earth Syst. Sci. Data*, 6, 69–90, doi:10.5194/essd-6-69-2014, 2014.
- Bauer, J. E., Cai, W.-J., Raymond, P. A., Bianchi, T. S., Hopkinson, C. S., and Regnier, P. A. G.: The changing carbon cycle of the coastal ocean, *Nature*, 504, 61–70, doi:10.1038/nature12857, 2013.
- Bianchi, A. A., Piola, A. R., Pino, D. R., Schloss, I., Poisson, A., and Balestrini, C. F.: Vertical stratification and air–sea CO_2 fluxes in the Patagonian Shelf, *J. Geophys. Res.*, 110, C07003, doi:10.1029/2004JC002488, 2005.
- Bianchi, A. A., Pino, D. R., Perlender, H. G. I., Osiroff, A. P., Segura, V., Lutz, V., Clara, M. L., Balestrini, C. F., and Piola, A. R.: Annual balance and seasonal variability of sea–air CO_2 fluxes in the Patagonia Sea: their relationship with fronts and chlorophyll distribution, *J. Geophys. Res.*, 114, C03018, doi:10.1029/2008JC004854, 2009.
- Cai, W.-J.: The role of marsh-dominated heterotrophic continental margins in transport of CO_2 between the atmosphere, the land–sea interface and the ocean, *Geophys. Res. Lett.*, 30, 1849, doi:10.1029/2003GL017633, 2003.
- Carton, J. A. and Giese, B. S.: A reanalysis of ocean climate using Simple Ocean Data Assimilation (SODA), *Mon. Weather Rev.*, 136, 2999–3017, 2008.
- Chen, C.-T. A., Huang, T.-H., Chen, Y.-C., Bai, Y., He, X., and Kang, Y.: Air–sea exchanges of CO_2 in the world’s coastal seas, *Biogeosciences*, 10, 6509–6544, doi:10.5194/bg-10-6509-2013, 2013.
- Ciais, P., Sabine, C., Bala, G., Bopp, L., Brovkin, V., Canadell, J., Chhabra, A., DeFries, R., Galloway, J., Heimann, M., Jones, C., Le Quéré, C., Myneni, R. B., Piao, S., and Thornton, P.: Carbon and other biogeochemical cycles, in: *Climate Change 2013: the Physical Science Basis, Contribution of Working Group I to the Fifth Assessment Report of the Intergovernmental Panel on Climate Change*, Cambridge University Press, Cambridge, UK and New York, NY, USA, 465–570, 2014.
- Da Silva, A., Young, C., and Levitus, S.: *Atlas of Surface Marine Data 1994*, vol. 1, Algorithms and Procedures, NOAA Atlas NESDIS 6, US Department of Commerce, NOAA, NESDIS, USA, p. 74, 1994.
- Dabrowski, T., Lyons, K., Berry, A., Cusack, C., and Nolan, G. D.: An operational biogeochemical model of the North-East Atlantic: model description and skill assessment, *J. Marine Syst.*, 129, 350–367, doi:10.1016/j.jmarsys.2013.08.001, 2014.
- Doney, S. C., Lima, I., Feely, R. A., Glover, D. M., Lindsay, K., Mahowald, N., Moore, J. K., and Wanninkhof, R.: Mechanisms governing interannual variability in upper-ocean inorganic carbon system and air–sea CO_2 fluxes: physical climate and atmospheric dust, *Deep-Sea Res. Pt. II*, 56, 640–655, doi:10.1016/j.dsr2.2008.12.006, 2009.
- Fennel, K. and Wilkin, J.: Quantifying biological carbon export for the northwest North Atlantic continental shelves, *Geophys. Res. Lett.*, 36, L18605, doi:10.1029/2009GL039818, 2009.
- Gonzalez-Silvera, A., Santamaria-del Angela, E., Garcia, V. M. T., Garcia, C. A. E., Millan-Nunez, R., and Muller-Karger, F.: Biogeographical regions of the tropical and subtropical Atlantic Ocean off South America: classification based on pigment (CZCS) and chlorophyll-*a* (SeaWiFS), *Cont. Shelf Res.*, 24, 983–1000, doi:10.1016/j.csr.2004.03.002, 2004.
- Gruber, N.: Ocean biogeochemistry: carbon at the coastal interface, *Nature*, 517, 148–149, 2015.
- Gruber, N., Frenzel, H., Doney, S. C., Marchesiello, P., McWilliams, J. C., Moisan, J. R., Oram, J. J., Plattner, G.-K., and Stolzenbach, K. D.: Eddy-resolving simulation of plankton ecosystem dynamics in the California Current System, *Deep-Sea Res. Pt. I*, 53, 1483–1516, doi:10.1016/j.dsr.2006.06.005, 2006.
- Gruber, N., Lachkar, Z., Frenzel, H., Marchesiello, P., Münnich, M., McWilliams, J. C., Nagai, T., and Plattner, G.-K.: Eddy-induced reduction of biological production in eastern boundary upwelling systems, *Nat. Geosci.*, 4, 787–792, doi:10.1038/ngeo1273, 2011.
- Guerrero, R. A., Piola, A. R., Fenco, H., Matano, R. P., Combes, V., Chao, Y., James, C., Palma, E. D., Saraceno, M., and Strub, P. T.: The salinity signature of the cross-shelf exchanges in the Southwestern Atlantic Ocean: satellite observations, *J. Geophys. Res.-Oceans*, 119, 7794–7810, 2014.
- Hauri, C., Gruber, N., Vogt, M., Doney, S. C., Feely, R. A., Lachkar, Z., Leinweber, A., McDonnell, A. M. P., Münnich, M., and Plattner, G.-K.: Spatiotemporal variability and long-term

- trends of ocean acidification in the California Current System, *Biogeosciences*, 10, 193–216, doi:10.5194/bg-10-193-2013, 2013.
- Hofmann, E. E., Cahill, B., Fennel, K., Friedrichs, M. A. M., Hyde, K., Lee, C., Mannino, A., Najjar, R. G., O'Reilly, J. E., Wilkin, J., and Xue, J.: Modeling the dynamics of continental shelf carbon, *Ann. Rev. Mar. Sci.*, 3, 93–122, doi:10.1146/annurev-marine-120709-142740, 2011.
- Ito, R., Schneider, B., and Thomas, H.: Distribution of surface *f*CO₂ and air–sea fluxes in the Southwestern subtropical Atlantic and adjacent continental shelf, *J. Marine Syst.*, 56, 227–242, doi:10.1016/j.jmarsys.2005.02.005, 2005.
- Kantha, L.: Barotropic tides in the global oceans from a non-linear tidal model assimilating altimetric tides: 1. Model description and results, *J. Geophys. Res.-Oceans*, 100, 283–308, doi:10.1029/95JC02578, 1995.
- Körtzinger, A.: Determination of carbon dioxide partial pressure (*p*(CO₂)), in: *Methods of Seawater Analysis*, 3rd edn., 149–158, 1999.
- Landschützer, P., Gruber, N., Bakker, D., and Schuster, U.: Recent variability of the global ocean carbon sink, *Global Biogeochem. Cy.*, 28, 927–949, 2014.
- Laruelle, G. G., Dürr, H. H., Lauerwald, R., Hartmann, J., Slomp, C. P., Goossens, N., and Regnier, P. A. G.: Global multi-scale segmentation of continental and coastal waters from the watersheds to the continental margins, *Hydrol. Earth Syst. Sci.*, 17, 2029–2051, doi:10.5194/hess-17-2029-2013, 2013.
- Laruelle, G. G., Lauerwald, R., Pfeil, B., and Regnier, P.: Regionalized global budget of the CO₂ exchange at the air–water interface in continental shelf seas, *Global Biogeochem. Cy.*, 28, 1199–1214, 2014.
- Lovenduski, N. S., Gruber, N., Doney, S. C., and Lima, I. D.: Enhanced CO₂ outgassing in the Southern Ocean from a positive phase of the Southern Annular Mode, *Global Biogeochem. Cy.*, 21, GB2026, doi:10.1029/2006GB002900, 2007.
- Millero, F.: Thermodynamics of the carbon dioxide system in the oceans, *Geochim. Cosmochim. Ac.*, 59, 661–677, 1995.
- Moore, J. K., Lindsay, K., Doney, S. C., Long, M. C., and Misumi, K.: Marine ecosystem dynamics and biogeochemical cycling in the Community Earth System Model [CESM1 (BGC)]: Comparison of the 1990s with the 2090s under the RCP4. 5 and RCP8. 5 scenarios, *J. Climate*, 26, 9291–9312, 2013.
- Muller-Karger, F. E., Varela, R., Thunell, R., Luerssen, R., Hu, C., and Walsh, J. J.: The importance of continental margins in the global carbon cycle, *Geophys. Res. Lett.*, 32, L01602, doi:10.1029/2004GL021346, 2005.
- Nash, J. and Sutcliffe, J.: River flow forecasting through conceptual models Part I – a discussion of principles, *J. Hydrol.*, 10, 282–290, 1970.
- Ospar, V. M., De Vries, I., Bokhorst, M., Ferreira, J., Gellers-Barkmann, S., Kelly-Gerreyn, B., Lancelot, C., Mensguen, A., Moll, A., Pätsch, J., Radach, G., Skogen, M., Soiland, H., Svendsen, E., and Vested, H. J.: Report of the ASMO Modelling Workshop on Eutrophication Issues, The Hague, the Netherlands, 5–8 November 1996, OSPAR Commission Report, 102, 90, 1998.
- Piola, A. and Matano, R.: Brazil and Falklands (Malvinas) currents, in: *Ocean Currents: a Derivative of the Encyclopedia of Ocean Sciences*, 35–43, 2001.
- Rippeth, T., Lincoln, B., Kennedy, H., Palmer, M., Sharples, J., and Williams, C.: Impact of vertical mixing on sea surface *p*CO₂ in temperate seasonally stratified shelf seas, *J. Geophys. Res.-Oceans*, 119, 3868–3882, 2014.
- Risien, C. M. and Chelton, D. B.: A global climatology of surface wind and wind stress fields from eight years of QuikSCAT scatterometer data, *J. Phys. Oceanogr.*, 38, 2379–2413, 2008.
- Saraceno, M., D'Onofrio, E., Fiore, M., and Grismeyer, W.: Tide model comparison over the Southwestern Atlantic Shelf, *Cont. Shelf Res.*, 30, 1865–1875, doi:10.1016/j.csr.2010.08.014, 2010.
- Sarmiento, J. and Gruber, N.: *Ocean Biogeochemical Dynamics*, Princeton University Press, Princeton, NJ, USA, 2006.
- Shchepetkin, A. and McWilliams, J.: The regional oceanic modeling system (ROMS): a split-explicit, free-surface, topography-following-coordinate oceanic model, *Ocean Model.*, 9, 347–404, 2005.
- Signorini, S. R., Mannino, A., Najjar, R. G., Friedrichs, M. A. M., Cai, W.-J., Salisbury, J., Wang, Z. A., Thomas, H., and Shadwick, E.: Surface ocean *p*CO₂ seasonality and sea–air CO₂ flux estimates for the North American east coast, *J. Geophys. Res.-Oceans*, 118, 5439–5460, doi:10.1002/jgrc.20369, 2013.
- Stow, C. A., Jolliff, J., McGillicuddy, D. J., Doney, S. C., Allen, J. I., Friedrichs, M. A., Rose, K. A., and Wallhead, P.: Skill assessment for coupled biological/physical models of marine systems, *J. Marine Syst.*, 76, 4–15, 2009.
- Takahashi, T., Sutherland, S. C., Sweeney, C., Poisson, A., Metzl, N., Tilbrook, B., Bates, N., Wanninkhof, R., Feely, R. A., Sabine, C., Olafsson, J., and Nojiri, Y.: Global sea–air CO₂ flux based on climatological surface ocean *p*CO₂, and seasonal biological and temperature effects, *Deep-Sea Res. Pt. II*, 49, 1601–1622, 2002.
- Takahashi, T., Sutherland, S. C., Wanninkhof, R., Sweeney, C., Feely, R. A., Chipman, D. W., Hales, B., Friederich, G., Chavez, F., Sabine, C., Watson, A., Bakker, D. C. E., Schuster, U., Metzl, N., Yoshikawa-Inoue, H., Ishii, M., Midorikawa, T., Nojiri, Y., Körtzinger, A., Steinhoff, T., Hoppema, M., Olafsson, J., Arnarson, T. S., Tilbrook, B., Johannessen, T., Olsen, A., Bellerby, R., Wong, C. S., Delille, B., Bates, N. R., and de Baar, H. J. W.: Climatological mean and decadal change in surface ocean *p*CO₂, and net sea–air CO₂ flux over the global oceans, *Deep-Sea Res. Pt. II*, 56, 554–577, 2009.
- Tsunogai, S., Watanabe, S., and Sato, T.: Is there a “continental shelf pump” for the absorption of atmospheric CO₂?, *Tellus B*, 51, 701–712, doi:10.1034/j.1600-0889.1999.t01-2-00010.x, 1999.
- Turi, G., Lachkar, Z., and Gruber, N.: Spatiotemporal variability and drivers of *p*CO₂ and air–sea CO₂ fluxes in the California Current System: an eddy-resolving modeling study, *Biogeosciences*, 11, 671–690, doi:10.5194/bg-11-671-2014, 2014.
- Walsh, J.: Importance of continental margins in the marine biogeochemical cycling of carbon and nitrogen, *Nature*, 350, 53–55, 1991.
- Wang, A. Z., Cai, W.-J., Wang, Y., and Ji, H.: The southeastern continental shelf of the United States as an atmospheric CO₂ source and an exporter of inorganic carbon to the ocean, *Cont. Shelf Res.*, 25, 1917–1941, doi:10.1016/j.csr.2005.04.004, 2005.
- Yool, A. and Fasham, M.: An examination of the “continental shelf pump” in an open ocean general circulation model, *Global Biogeochem. Cy.*, 15, 831–844, doi:10.1029/2000GB001359, 2001.